EURASIAN PHYSICAL TECHNICAL JOURNAL

2026, Volume 23, No. 2 (56)

https://doi.org/10.31489/2026N2/118-129

Received: 24/01/2026 Revised: 31/05/2026 Accepted: 26/06/2026 Published online: 30/06/2026

Original Research Article

UDC 538.911

STUDY OF CRYOVACUUM CONDENSATES OF A CARBON MONOXIDE, CARBON DIOXIDE AND METHANE MIXTURES WITH WATER IN A 95:5 RATIO

Chigambayeva N.N., Nurmukan A.Y., Aldiyarov A.U., Korshikov E.S., Erlanov T.E.

Al-Farabi Kazakh National University, Almaty, Kazakhstan
*Corresponding author: nurgul050490@gmail.com

Abstract. *In the context of the intensifying greenhouse effect, the search for effective approaches to the capture and retention of greenhouse gases such as CO, CO_2, and CH_4 has become increasingly relevant. The aim of the present work is to experimentally investigate the absorption capacity of water cryocrystals with respect to CO, CO_2, and CH_4 molecules under low-temperature and vacuum conditions, as well as to analyze the effect of phase transitions of water ice on the kinetics of gas impurity release from the standpoint of the prospective application of these systems in decarbonization technologies. This work presents experimental results on the investigation of the absorption properties of water cryocrystals with respect to CO, CO_2, and CH_4 molecules under deep vacuum and ultra-low temperature conditions (13–200 K). Using temperature-programmed desorption (TPD), mass spectrometry (MS), and laser interferometry, the ability of water ice in various phase states (amorphous, cubic, and hexagonal) to efficiently retain and stepwise release gas impurities has been demonstrated. A correlation between the phase transitions of ice (ASW → Ic → Ih) and the desorption behavior of the molecules has been established. The obtained results confirm the potential of water cryostructures for use as passive or controllable sorbents within prospective decarbonization technologies, environmental monitoring, and gas storage applications.*

Keywords: low temperature, temperature-programmed desorption, mass spectrometry, cryogenic conditions, carbon dioxide, carbon monoxide, methane.

1. Introduction

Global climate change is driven by the increase in anthropogenic emissions of greenhouse gases, primarily carbon monoxide (CO), carbon dioxide (CO_2), and methane (CH_4), whose atmospheric concentrations have reached record levels over the entire period of instrumental observations [1]. CO and CO_2 account for the major share of radiative forcing, whereas CH_4 exhibits a significantly higher global warming potential per unit mass, making both gases key targets of climate policy and scientific research [2,3].

According to estimates by the Intergovernmental Panel on Climate Change (IPCC), without additional emission reduction measures, global temperature increases by the end of the 21st century could exceed 3 °C, posing serious risks to sustainable development [4]. According to the International Energy Agency (IEA), global carbon dioxide emissions from the energy sector have exhibited a steady upward trend during the period 2020–2024. After decreasing to 34.2 Gt in 2020 due to reduced economic activity during the COVID-19 pandemic, emissions sharply increased to 36.3 Gt in 2021. In the subsequent years (2022–2024), the growth rate slowed; however, the total emissions reached 37.6 Gt, representing a 9.7 % increase compared to 2020, as shown in Figure 1. This increase is primarily associated with the growth in energy consumption in industry

and transportation, despite the active deployment of renewable energy sources. At the same time, according to IEA estimates, the development of low-carbon technologies has prevented an additional approximately 2.5 Gt of CO_2 emissions per year [5, 6].

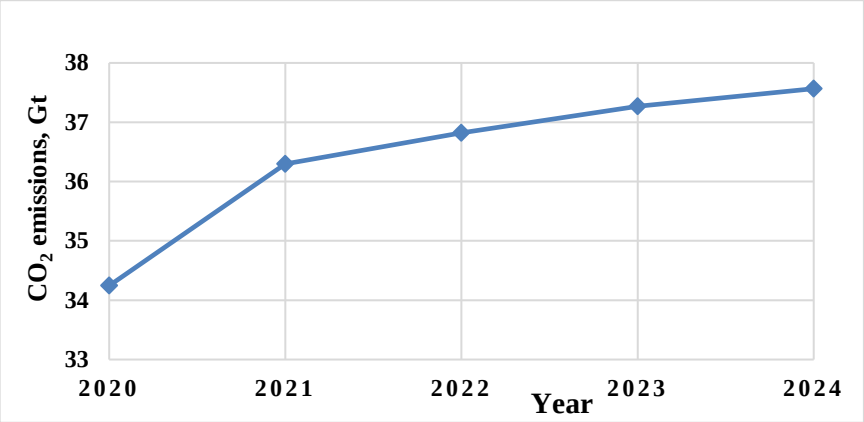

Fig. 1. Analysis of global CO_2 emissions dynamics based on IEA data (2020–2024) [5, 6]

The increase in greenhouse gas emissions observed in recent years indicates that existing measures are insufficient to achieve climate targets, making decarbonization policy particularly relevant. Under current conditions, decarbonization is not only an environmental measure but also a strategic necessity in the context of the escalating climate crisis, requiring active participation of industrial enterprises in reducing their carbon footprint through improved energy efficiency, modernization of technological processes, and implementation of innovative solutions [7]. As noted in [8], an important component of this strategy is the capture, storage, and utilization of CO_2, including its use for biofuel production, which contributes to sustainable development. In this context, alongside the transition to renewable energy sources, carbon capture, storage, and utilization technologies (CCS/CCU) are gaining increasing significance, being considered a necessary and complementary approach within the framework of energy and industrial decarbonization [9, 10].

Traditional methods for capturing CO, CO_2, and CH_4, including chemical and physical absorption, adsorption on porous materials, and membrane technologies, face several limitations related to high energy consumption, material degradation, and significant operational costs [11–13]. This motivates the search for alternative approaches capable of providing high purification efficiency while reducing both energy and economic expenditures [14].

Promising directions include cryogenic methods for gas capture and separation, which are based on phase transitions at low temperatures. Recent studies indicate that cryogenic technologies can be effective when working with gas mixtures containing high concentrations of CO, CO_2, and CH_4, as well as when integrated with gas liquefaction and storage processes [10, 14, 15]. At the same time, the further development and optimization of such technologies are impossible without a detailed understanding of the molecular mechanisms governing gas–condensed phase interactions, as well as an analysis of their phase and structural behavior under cryogenic conditions, which necessitates the use of highly sensitive experimental techniques.

Infrared (IR) spectroscopy methods play a key role in advancing experimental research in low-temperature physics and gas-phase chemistry, as they enable the investigation of the molecular state of substances and their interactions with the condensed phase at cryogenic temperatures. In particular, a low-temperature measurement cell for IR spectroscopy of hydrocarbon materials has been developed and experimentally validated, operating in the temperature range of 77–300 K at atmospheric pressure. This approach makes it possible to obtain new fundamental data on molecular behavior under cryogenic conditions. Such experimental methodologies are also of considerable interest for studying cryovacuum condensates and cryogenic gas capture processes, as they provide precise control over temperature effects, phase transitions, and the spectral characteristics of molecules confined within low-temperature water-based structures [16]. Within this approach, particular interest is drawn to water cryostructures, including cryovacuum condensates and gas hydrates, in which gas molecules are encapsulated within the crystalline lattice of water [17, 18].

Gas hydrate and clathrate systems are actively investigated both for CO_2 capture and storage and for the replacement of methane in natural hydrate deposits, offering opportunities for simultaneously addressing

climate and energy challenges [12, 13, 17]. However, the practical application of these technologies requires a thorough understanding of the processes of gas sorption and temperature-dependent desorption, the phase behavior of water ice, and the kinetics of structural transitions under cryogenic conditions [15, 18].

Recent studies have demonstrated that amorphous solid water (ASW) possesses a highly porous structure capable of effectively trapping volatile molecules within an interconnected network of nanopores. The porosity and gas-retention capacity of ASW are strongly dependent on deposition conditions and thermal history. Upon annealing, ASW undergoes progressive pore collapse, structural densification, and crystallization, all of which significantly influence the release kinetics of trapped gases. Experimental studies have shown that heating ASW results in pore closure, confinement of gases within isolated cavities, and subsequent desorption associated with structural relaxation and crystallization of the ice matrix. These processes are of considerable importance for cryogenic gas storage, the evolution of astrophysical ices, and low-temperature adsorption phenomena. Recent neutron-scattering investigations have provided direct evidence of pore restructuring and densification in ASW during heating, further confirming the strong relationship between ice morphology and the retention of volatile species. Therefore, the study of gas trapping and release in amorphous solid water remains an important research area for understanding the mechanisms of molecular transport and storage in cryogenic water-based systems [19 - 22].

2. Methodology and Experimental Setup

2.1 Experimental Apparatus

In this study, a universal vacuum spectrophotometer was used to perform experiments on cryocondensed films. The working chamber of the setup was evacuated using a rotary vane pump and a turbomolecular pump. A pressure of approximately P ~ 10^{-4} Torr was achieved during preliminary evacuation, while pressures of ~10^{-8} Torr were attained in the high-vacuum measurement mode. A detailed description of the experimental setup used is provided in [23]. The schematic diagram of the experimental setup used in this work is shown in Figure 2. Gradual annealing of the samples was carried out using a DT-670 semiconductor temperature sensor, whose operation was controlled by an LS325 temperature controller (Lake Shore, USA). Experimental data were analyzed using the temperature-programmed desorption (TPD) method. The samples were heated at a constant rate of dT/dt = 0.166 K/s while maintaining high vacuum conditions of approximately ~10^{-8} Torr.

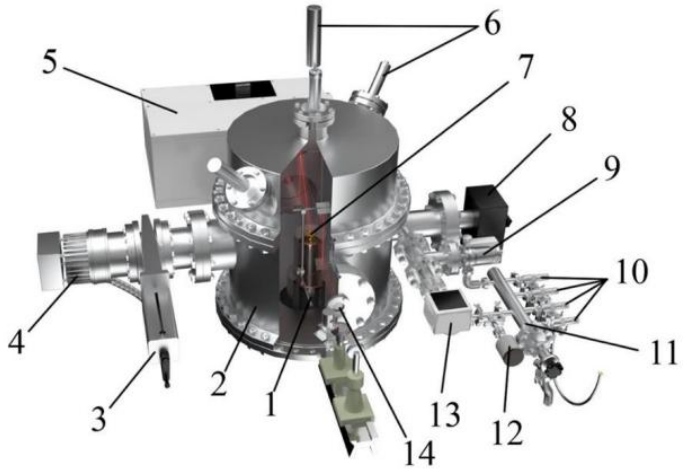

Fig. 2. Schematic diagram of the cryovacuum spectrophotometer setup: 1 – cryostat; 2 – vacuum chamber; 3 – rotary vane pump; 4 – turbomolecular pump; 5 – Fourier-IR spectrometer; 6 – dual-beam laser interferometer; 7 – substrate; 8 – mass spectrometer; 9 – dosing valves; 10 – manometers and pressure sensors [23]

Temperature control was achieved with an accuracy of ±0.1 K over the range of 13–310 K. A copper plate coated with a thin layer of high-purity gold (99.99%) was used as the substrate and cooled to cryogenic temperatures, providing efficient condensation of the gas-phase components. A combination of TPD-MS methods was employed to analyze the desorption of components from cryocondensed films. During programmed heating, the mass spectra of desorbing components as well as the overall pressure change in the working chamber were recorded. This approach allowed us to determine which molecules were released from

the substrate surface and at which temperatures their desorption occurred. The resulting TPD curves reflected the intensity of gas release from the substrate surface as a function of temperature.

2.2 Material

Samples of condensed mixtures of the H_2O–gas system (CO, CO_2, CH_4) were prepared by physical vapor deposition (PVD) at a substrate temperature of T = 13 K and a chamber pressure of approximately P ~ 10^{-4} Torr. The gas mixture was prepared by simultaneously introducing saturated water vapor and the gaseous impurity into the working volume of the chamber through dosing valves. The component ratio in the mixture was 95:5 (H_2O:gas). Distilled water with a residual impurity content of less than 0.005% was used as one of the main components, along with CO_2 of 99.999% purity (ISKHAN TEKHNO-GAZ LLC, Almaty, Kazakhstan), as well as CO and CH_4 with a purity of 99.95%.

2.3 Measurement methodology

The film thickness $d$was determined from the interference pattern recorded by a dual-beam laser interferometer, according to the relation:

$$d = \frac{m\lambda}{2ncos\theta} \ , \tag{1}$$

where: m — the number of interference fringes, λ= 405 nm — the laser wavelength, n — the refractive index of ice, θ — the angle of incidence of the laser beam.

A dual-beam laser interferometer was used to evaluate the thickness, density, and optical properties of the condensed films. Laser sources with a wavelength of λ = 405 nm were oriented at angles of α_1 = 1° and α_2 = 45° relative to the substrate surface. The geometry of the dual-beam laser interferometer and the arrangement of the laser beam relative to the substrate are shown in Figure 3. Mass spectra were recorded with a time step of 4 s over the mass-to-charge range of m/z = 1–100.

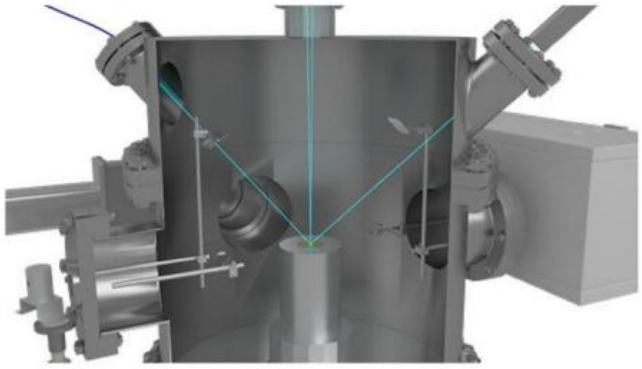

Fig. 3. Three-dimensional model of the experimental setup showing the direction of laser beams [19]

The experimental data were analyzed using the specialized software package EASY, developed for this work. The software enabled signal filtering, automatic peak detection, construction of mass–temperature profiles, and export of processed data for subsequent analysis and visualization. This approach facilitated efficient processing of large datasets and the determination of the quantitative characteristics presented below.

3. Results and Discussion

3.1 Absorption Capacity of Water Cryocrystals for CO, CO_2, and CH_4 Molecules

In this study, the absorption capacity of water cryocrystals with respect to CO, CO_2, and CH_4 molecules was investigated based on the analysis of the temperature-programmed desorption (TPD) of impurities from water ice films during controlled annealing. Two complementary approaches were employed to study the processes of gas molecule retention within the crystalline lattice: a manometric method (recording the total pressure) and a mass spectrometric method (identification of individual components). In parallel with the desorption measurements, optical monitoring of structural changes in the ice matrix was performed, allowing

the correlation between the absorption capacity of ice and its crystalline structure to be established. Each process of impurity molecule retention was considered separately.

Table 1. Comparison of the present results with previously experimental studies on amorphous solid water (ASW)

№	Reference	Ice system	Gas / Sample	Experimental method	Main desorption / structural transition temperature (K)	Main findings
1	This work	ASW + CO, CO_2, CH_4	H_2O–gas mixture	TPD, MS, Laser interferometry	13-200	Three desorption stages associated with ASW - Ic - Ih structural transformations. Excellent agreement between pressure, mass spectrometric and optical measurements.
2	Amato et al. (2025)	Porous ASW	H_2O ASW	Molecular dynamics simulation	15–160	Progressive pore collapse and ice densification during annealing [26].
3	Talewar et al. (2019)	Vapor-deposited ASW	Ar, CH_4, CO_2, He	TPD, Mass Spectrometry	95–185	Identified three gas-release mechanisms: desorption from cracks (>100 K), pore collapse (~125 K), and gas release during crystallization (~155 K) [20].
4	Yuan, Smith & Kay (2016)	ASW films	H_2O	TPD, RAIRS	150–160	Surface-initiated top-down crystallization [24].
5	Mate et al. (2020)	Porous ASW	CH_4/H_2O	FTIR, (QCM), Monte Carlo simulation	42–60	CH_4 diffusion depends on ASW morphology; porous interconnected structures enhance low-temperature gas trapping [25].

Table 1 demonstrates that the results obtained in the present study are consistent with previously reported experimental and computational investigations of amorphous solid water (ASW). Earlier studies have shown that heating ASW leads to progressive pore collapse, structural densification, glass transition, and subsequent crystallization. These structural transformations strongly affect the retention and release of molecules trapped within the ice matrix.

In agreement with these studies, our temperature-programmed desorption experiments reveal that the release of CO, CO_2, and CH_4 occurs in several stages associated with the structural evolution of water ice. The observed desorption behavior confirms that the transformation of ASW into crystalline phases governs the mobility and escape of trapped gas molecules.

Unlike previous investigations, which mainly focused on the structural evolution of pure ASW, the present work examines a multicomponent H_2O–CO–CO_2–CH_4 cryocondensate. This extends the understanding of the relationship between ice phase transitions and gas-release kinetics, providing useful information for cryogenic gas storage, decarbonization technologies, and astrophysical ice analogues.

Figure 4 shows the temperature dependence of the gas pressure recorded during the heating of a thin ice film TPD containing impurity molecules. The curve represents the total desorption signal of all system components and exhibits three clearly defined gas release regions, each corresponding to different desorption processes.

Figure 5 presents the TPD results obtained using cyclic mass spectrometric scanning. Unlike the integral data shown in Figure 4, mass spectrometric analysis allowed the separate contribution of individual components (CO, CO_2, CH_4) to be recorded and enabled precise identification of the desorbing molecules.

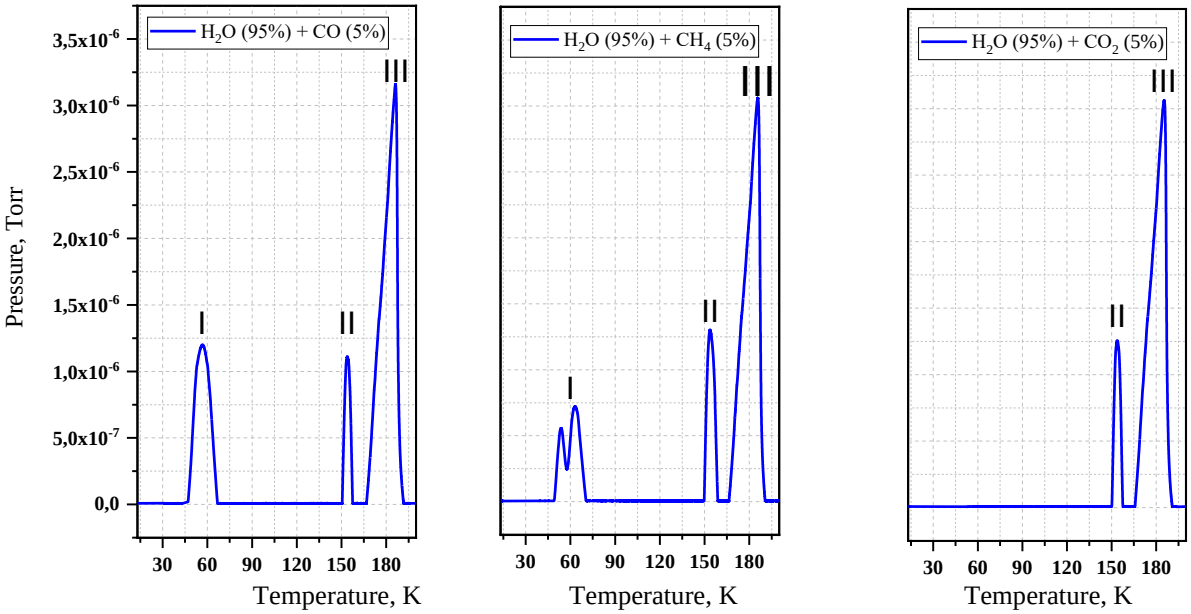

Fig. 4. Temperature-programmed desorption (according to pressure gauge readings) for various mixtures

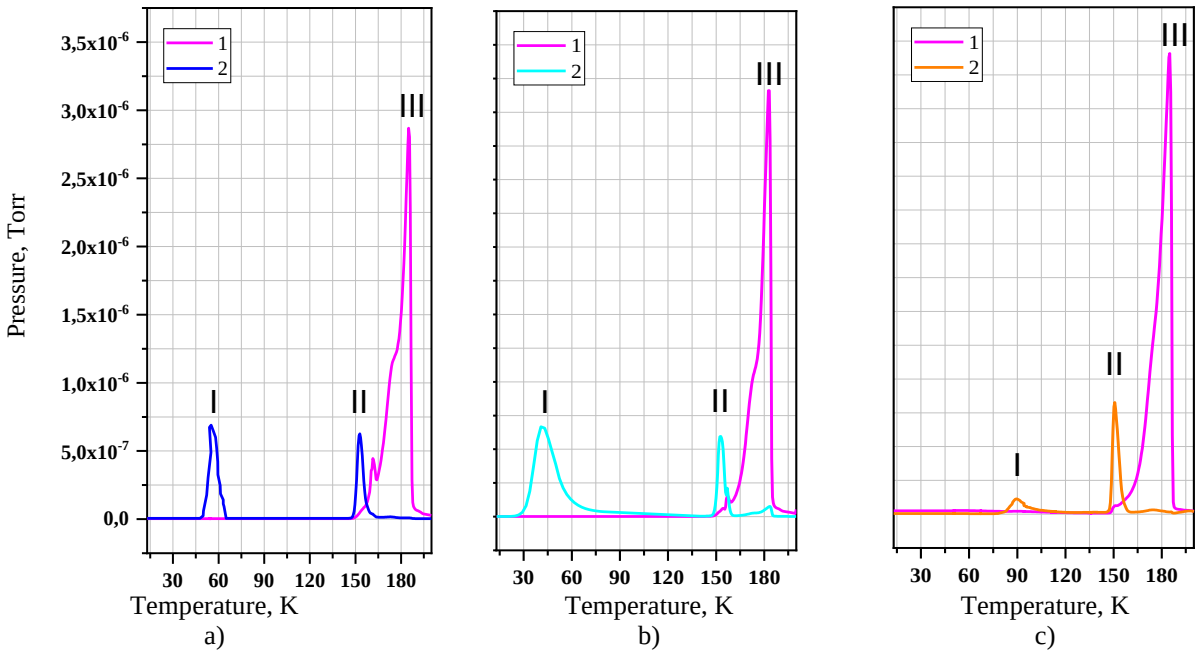

Fig. 5. Temperature-programmed desorption (mass spectrometry analysis, cyclic scanning) for various mixtures: 1 - H_2O (95 %), 2 (blue) – CO (5 %), 2 (cyan) - CH_4 (5 %), 2 (orange) - CO_2 (5 %)

Both applied methods—the manometric and the mass spectrometric—showed complete agreement in the results, revealing three distinctly identifiable regions of impurity molecule desorption from the ice matrix:

– *Low-temperature desorption region – I (40–140 K)*

In the first temperature range, desorption of the most weakly bound molecules are observed. The process includes the removal of physically adsorbed molecules from the ice surface and their release from the open pores of the amorphous ice structure. This stage is recorded by both methods—via manometric measurements (CO, CH_4) and mass spectrometric data (CO, CH_4, CO_2).

– *Medium-temperature range – II (140–160 K)*

This stage corresponds to the release of more strongly bound molecules from crystalline defects and their desorption from closed pores formed during the deposition and relaxation of amorphous ice. The process is

equally well manifested in the curves obtained by both methods, indicating the universality of this desorption process.

– *High-temperature region – III (>160 K)*

This stage corresponds to the desorption of the most strongly retained molecules, associated with the breakdown of residual supramolecular structures during the sublimation of water ice.

The good agreement between the manometric and mass spectrometric measurements confirms the consistency of the obtained desorption data.

3.2 Release of Impurity Molecules during Structural Transformations of Water Ice (ASW(L) → ASW(H))

Figure 6 presents optical study data demonstrating the release of impurity molecules CO, CH_4, CO_2 during the thermally induced densification of low-density amorphous ice. Two pronounced peaks are observed for CO and CH_4, along with a weaker peak for CO_2, indicating differences in the desorption dynamics of these gases. The differences in peak intensities reflect the varying sorption capacities of the water matrix toward these gases. Methane and carbon monoxide exhibit pronounced release at the early stages of heating, whereas carbon dioxide is released from the ice structure in significantly smaller amounts. The presented data clearly demonstrate distinct behaviors of the gas impurities during thermal processing of amorphous water ice. The primary factor determining the sequence of their release is the relationship between the thermal characteristics of the gases themselves and the structural changes in the ice matrix.

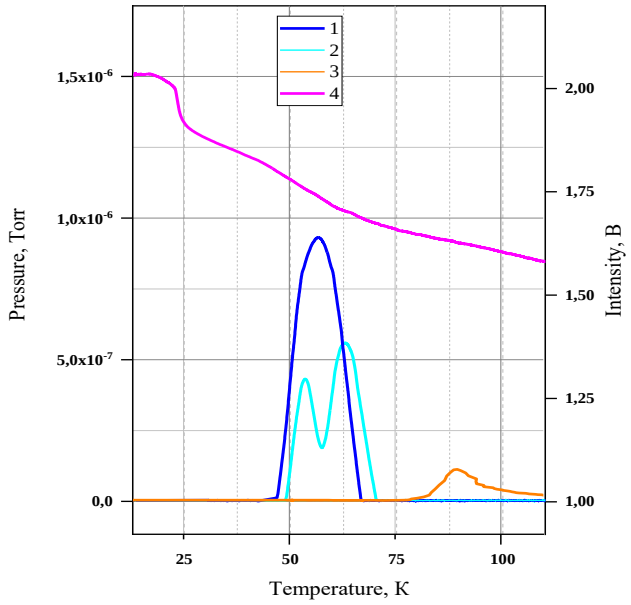

Fig. 6. Optical analysis of impurity molecule release during amorphous ice relaxation:
1 – CO (5 %), 2 - CH_4 ₂ (5 %), 3 - CO_2 (5 %), 4 - H_2O (95 %)

CH_4 and CO exhibit pronounced desorption peaks in the temperature range of 40–70 K. This behavior can be explained by the fact that their sublimation temperatures (34 K for CH_4 and 29 K for CO) are significantly lower than the temperature of intense pore collapse in amorphous ice (~70 K). As a result, these gases are released both through natural sublimation and during the relaxation of the ice structure. CO_2 behaves in a fundamentally different manner, exhibiting only weak signs of desorption within this temperature range. This behavior is due to its significantly higher sublimation temperature (80 K, Figure 7), which exceeds the temperature of intense pore collapse. As a result, CO_2 molecules remain securely trapped within the ice matrix until higher temperatures are reached.

The minor release of CO_2 in the low-temperature region can be attributed to two primary processes. First, surface desorption of molecules weakly bound to the outer layers of the ice film is possible. Second, a certain contribution may arise from the release of molecules from a limited number of macropores that remain after partial collapse of the porous structure. These assumptions are supported by the experimental data (Fig. 7),

which show a sharp, almost instantaneous release of CO_2 upon reaching its sublimation temperature—a behavior that is fundamentally different from the gradual desorption observed for CH_4 and CO.

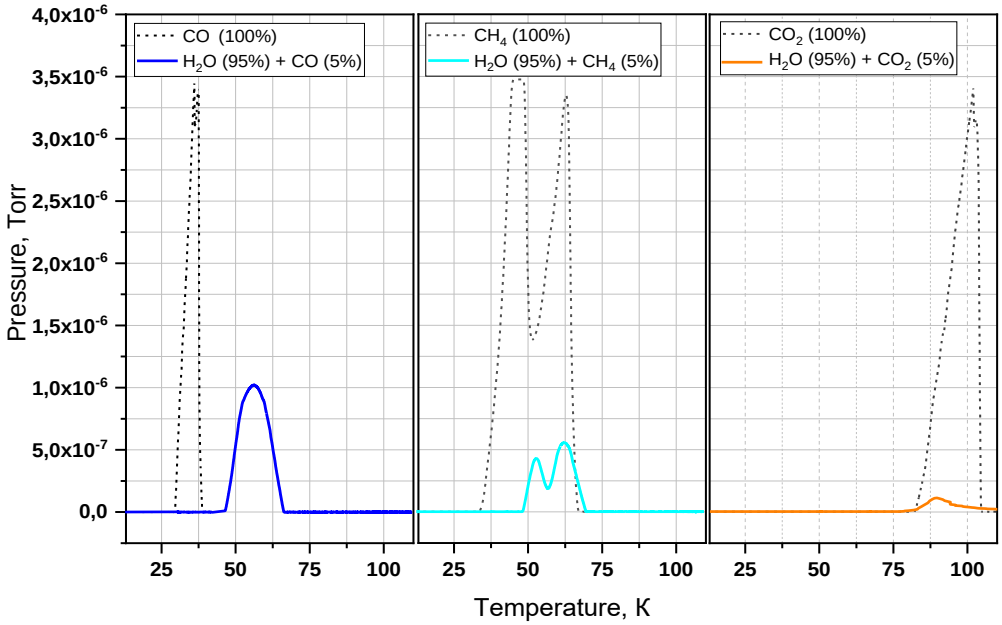

Fig. 7. Comparison of temperature profiles for the desorption of CH_4, CO, and CO_2 from amorphous ice film with the sublimation of pure substances

The results obtained demonstrate that gas desorption is determined by the combined effect of the gas sublimation temperature and structural transformations of the ice matrix. Gases with low sublimation temperatures (Ch_4 and CO) are released in the early stages of heating, while co_2 remains trapped until higher temperatures are reached. During the transition from ASW to Ic, crystallization causes pore compression, reduction of free volume, and elimination of structural defects, which leads to the release of impurity molecules trapped in the ice matrix. It is noteworthy that the desorption kinetics in this temperature range exhibit a complex behavior. In the initial stage of the transition (145–150 K), a gradual increase in the desorption rate is observed, corresponding to the activation of molecular mobility within the amorphous matrix. This is followed by a sharp jump in intensity (150–155 K), coinciding with the main phase of crystallization. During this period, cooperative rearrangement of large ice volumes occurs, leading to the simultaneous release of a significant number of impurities. The final stage of the process (155–160 K) is characterized by a gradual decrease in the desorption rate as crystallization completes.

3.3 Release of Impurity Molecules during Structural Transformations of Water Ice (Ic → Ih) and (ASW → Ih)

This section is devoted to the release of impurities during the structural transitions of water ice from the amorphous to the crystalline phase and during the recrystallization of Ic → Ih.

3.3.1 Optical Studies of Structural Transitions in Ice Films

Figure 8 shows the temperature dependence of the intensity of the laser signal, reflecting the structural transitions occurring in the ice film during heating.

Several key temperature intervals characterizing the structural transitions of ice are highlighted in the graph:

- *Interval I* – water remains in the form of amorphous ice (ASW), with the signal intensity remaining constant;
- *Interval II* – a sharp decrease in the laser signal intensity, associated with the transition of amorphous ice to the cubic modification (ASW → Ic);
- *Interval III* – a reduction in the slope of the curve due to the gradual transition of cubic ice into hexagonal ice (Ic → Ih), resulting from the similarity of their structural parameters.

- *Interval IV* – a sharp decrease in signal intensity, likely caused by the transformation of residual amorphous regions into the hexagonal structure (ASW → Ih), as confirmed by X-ray diffraction results;
- *Interval V* – continued growth of hexagonal ice crystals through the reorganization of remaining cubic regions, accompanied by a linear decrease in intensity;
- *Interval VI* – complete sublimation of the sample, during which the signal returns to its maximum value.

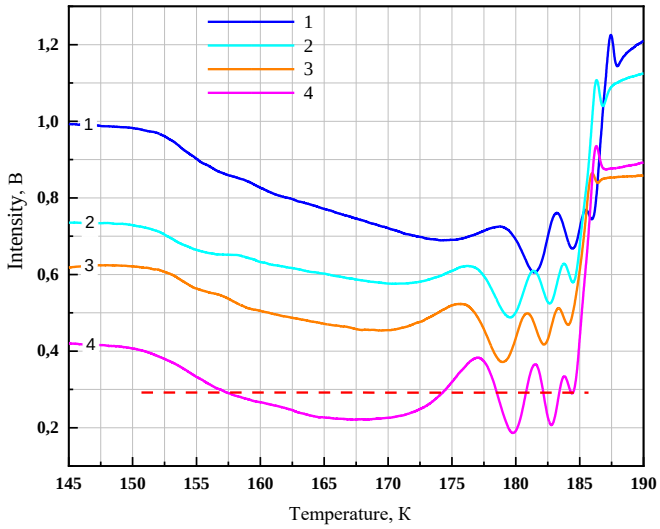

Fig. 8. Laser radiation intensity from the surface with a cryocondensate sample
1 – CO (5 %), 2 - CH_4 $_2$ (5 %), 3 - CO_2 (5 %), 4 - H_2O (95 %)

3.3.2Desorption of Impurities during Heating of the Thin Film

The mass spectrometric data presented in Figure 9 show clearly defined desorption peaks of impurities in the temperature range of 154–163 K (Intervals I and II), which correspond precisely to the regions of structural transitions III and IV in the temperature dependence of the laser signal intensity (Figure 8).

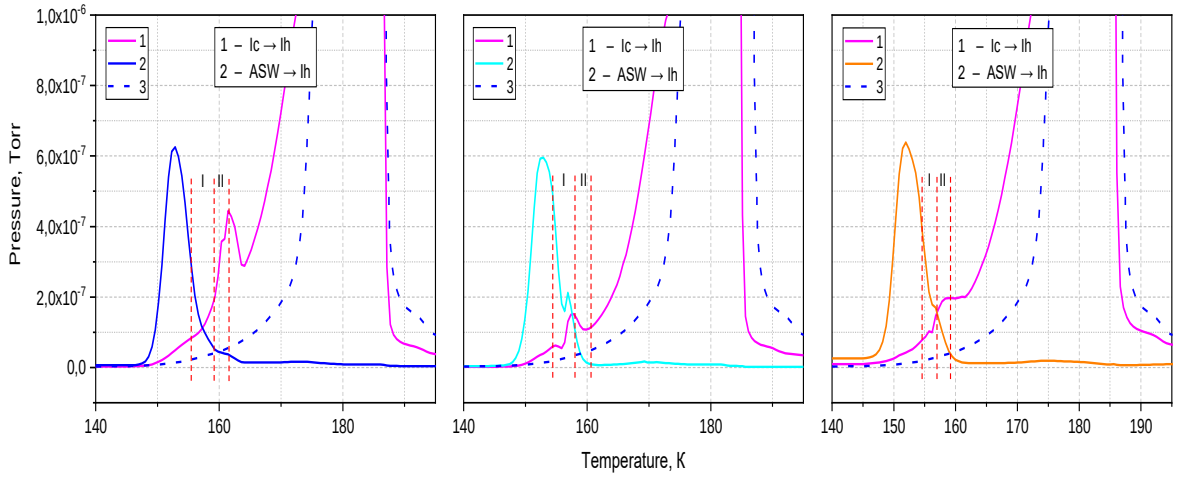

Fig. 9. Mass spectrometry desorption data as a function of temperature for water and various mixtures:
1 - H_2O (95 %), 2 – CO (5 %), 2 - CH_4 (5 %), 2 - CO_2 (5 %), 3 - H_2O (100 %)

The observed correlation indicates a direct relationship between the release of impurity molecules and the structural transformations in water ice during the heating of the thin film. The desorption peaks observed in Intervals I and II are attributed to structural transformations of the ice matrix during the Ic → Ih and ASW → Ih transitions. These processes involve defect elimination and pore collapse, which promote the release of impurity molecules trapped within the ice structure

3.3.3 Influence of the Molecular Mass of Impurities on Structural Transformations of Water Ice

Analysis of the influence of various impurities on the structural transitions of water ice demonstrates the key role of their molecular mass. Light molecules, such as methane (CH_4), due to their high mobility, interact actively with the crystalline lattice of water ice, efficiently transferring energy to it. This leads to localized heating in regions containing impurities, thereby facilitating the initiation of structural transitions. In particular, methane significantly affects the transformation of cubic (Ic) and residual amorphous (ASW) ice into the hexagonal (Ih) phase, accelerating this process within the corresponding temperature range, as confirmed by experimental data showing a shift in the phase transition temperature boundaries in the presence of methane.

Heavier molecules, such as CO_2, although less mobile, possess greater mass, allowing them to transfer more energy per collision; this higher energy transfer compensates for their lower mobility, resulting in a similar influence on ice structural transitions as observed for methane. CO occupies an intermediate position in terms of mass: it is heavier than methane but lighter than carbon dioxide. Consequently, its effect on the water ice structure is less pronounced than that of CH_4 and CO_2, as evidenced by minimal changes in the phase transition temperature boundaries when CO is present. It should be noted that, alongside molecular mass, the specific interactions of impurities with the hydrogen-bond network of ice may also contribute; however, within the scope of this study, the dominant factor is the molecular mass.

3.3.4 Uncertainty Analysis and Experimental Data Reliability

The reliability of the experimental results was assessed based on the stability of the experimental conditions and the consistency of the applied measurement techniques. Temperature control was performed using a DT-670 semiconductor sensor operated by a Lake Shore LS325 controller with an accuracy of ±0.1 K. Throughout all experiments, the heating rate was maintained constant at 0.166 K s^{-1}, minimizing thermal fluctuations during temperature-programmed desorption measurements.

The thickness of the cryocondensed films was determined by laser interferometry. The uncertainty of the thickness determination was mainly associated with interference fringe counting and the optical parameters of the ice film. However, this uncertainty did not affect the determination of desorption temperatures or the qualitative interpretation of the experimental results.

The desorption behavior of the samples was simultaneously monitored by three independent techniques: pressure measurements, mass spectrometry, and laser interferometry. The coincidence of the characteristic desorption temperature ranges obtained by these methods confirms the consistency and reliability of the experimental data. Minor differences in signal intensity are attributed to the different sensitivities of the measuring techniques and do not influence the identification of the desorption stages or the interpretation of the structural transformations of the ice matrix.

Overall, the combination of independent measurement methods, stable experimental conditions, and precise temperature control ensures the high reliability and reproducibility of the obtained results.

4. Conclusion

This study investigates the processes of adsorption and release of CO, CO_2, and CH_4 molecules in structures of cryocondensed water ice, in line with the main objective of the article — to elucidate the physical principles underlying the prospective cryotrapping of gases in water matrices. The use of a combination of manometric, mass spectrometric, and optical methods ensured the reliability and consistency of the obtained data. Gas desorption from the ice matrix occurs as a multistage process across three distinct temperature regions, each corresponding to different impurity retention mechanisms. It was established that structural transformations of water ice play a key role in gas release: transitions from the amorphous phase to cubic and hexagonal forms are accompanied by the collapse of the porous structure and the elimination of crystal lattice defects, resulting in intensive desorption of trapped molecules. The sequence and intensity of desorption are determined by the relationship between ice structural transformation temperatures and the sublimation temperatures of the gases: CH_4 and CO molecules are predominantly released at the early stages of heating, whereas CO_2 remains trapped until higher temperatures.

The precise agreement of desorption temperature boundaries obtained by different measurement techniques confirms the reproducibility of the results, the validity of the proposed desorption model, and the universality of molecular release processes from the ice matrix. Minor quantitative differences in peak

intensities do not affect the qualitative interpretation of the data, and the overall consistency of the experiments provides a reliable basis for analyzing the role of structural transformations of ice in gas desorption processes.

Thus, the obtained results demonstrate the effectiveness of cryocondensed water structures for selective gas capture and can serve as an experimental basis for the development of greenhouse gas cryotrapping technologies within the framework of decarbonization efforts.

Conflict of interest statement
The authors declare that they have no conflict of interest in relation to this research, whether financial, personal, authorship or otherwise, that could affect the research and its results presented in this paper.

CRediT author statement
Chigambayeva N.N.: Investigation, Writing-Original draft preparation, Editing; **Nurmukan A.Y.**: Writing Reviewing, Supervision; **Aldiyarov A.U.**: Conceptualization, Funding acquisition; **Yerlanov T.E.**: Resources, Software, Data curation, Methodology; **Korshikov E.S.**: Investigation, Visualization, Validation, **Erlanov T.E.:** Investigation, Writing-Original draft preparation. The final manuscript was read and approved by all authors.

Statement on the use of Artificial Intelligence.
During the preparation of this manuscript, artificial intelligence tools were used solely for language editing and grammatical improvement. No AI tools were used to generate scientific content, analysis, results, or conclusions.

Data Availability Statement
The data are available upon reasonable request from the authors.

Funding

This research was funded by the Committee of Science of the Ministry of Science and Higher Education of the Republic of Kazakhstan (Grant No. BR34636830).

References

1 World Meteorological Organization. (2022). Greenhouse gas concentrations reach record levels. WMO. https://wmo.int/ru/news/media-centre/koncentraciya-parnikovykh-gazov-dostigla-rekordnogo-urovnya-vnov

2 Lu, G., Zhang, Y., Li, X., Wang, J. (2023). Recent progress in carbon dioxide capture technologies: A comprehensive review. *Int. J. Environ. Sci. Technol. (IJEST)*. 1(1). https://doi.org/10.18686/cest.v1i1.32

3 Irgibayeva, I.S., Nurzhanova, A.K., Kassenova, Z.K. (2022). Climate change and the greenhouse effect. *Bulletin of ENU* 138(1), 18–23. https://doi.org/10.32523/2616-6771-2022-138-1-18-23

4 Intergovernmental Panel on Climate Change. (2018). *Global Warming of 1.5 °C*. Geneva: World Meteorological Organization. IPCC. https://www.ipcc.ch/sr15/

5 International Energy Agency. (2021). *Global Energy Review: CO_2 emissions in 2021*. IEA. https://www.iea.org/reports/global-energy-review-co2-emissions-in-2021

6 International Energy Agency. (2025). *Global Energy Review 2025*. https://www.iea.org/reports/global-energy-review-2025

7 Eurovent Certification. (2023). How do we decarbonise the HVAC manufacturing industry? https://www.eurovent-certification.com/ru/category/article/how-do-we-decarbonise-the-hvac-manufacturing-industry

8 Rahman, F.A., Maniruzzaman, M., Aziz, A., Saidur, R., Bakar, W.A.W.A., Hainin, M.R., Putrajaya, R., Hassan N.A. (2017). Pollution to solution: Capture and sequestration of carbon dioxide (CO_2) and its utilization as a renewable energy source for a sustainable future. *Renew. Sust. Energy Rev.* 71, 112–126. https://doi.org/10.1016/j.rser.2017.01.011

9 Font-Palma, C., Cann, D., Udaeta, M. (2021). Review of cryogenic carbon capture innovations and their potential applications. Carbon Capture Innovations and Their Potential Applications, 7(3), 58. https://www.mdpi.com/2311-5629/7/3/58

10 Kumar, S., Sharma, A., Singh, R. (2022). Review: CO_2 capturing methods of the last two decades. *Int. J. Environ. Sci. Technol. (IJEST)*. 20, 8087-8104. https://link.springer.com/article/10.1007/s13762-022-04680-0

11 Rahman, F.A., Aziz, A., Saidur R. (2017). Capture and sequestration of carbon dioxide and its utilization. *Renew. Sust. Energy Rev.* 71, 112–126. https://doi.org/10.1016/j.rser.2017.01.011

12 Pei, J., Zhang, L., Wang, Q. (2024). CO_2 capture technology based on gas hydrate method: A review. *Front. Chem.*, 12. https://doi.org/10.3389/fchem.2024.1448881

13 Rukh, M., Rahman, Md Sh., Sakib, K M N. (2024). A comprehensive review of semi-clathrate hydrates for CO_2 capture: Characterizations, mechanism and role of promoters. *Sep. Sci. Technol.*, 12, 100217. https://www.sciencedirect.com/science/article/pii/S2772656824000290

14 Tuinier, M.J., Annaland, M., Kuipers, J.A.M. (2010). Cryogenic CO_2 capture using dynamically operated packed beds. *Chem. Eng. Sci.*, 65, 114–125. https://doi.org/10.1016/j.ces.2009.01.055

15 Aneesh, A.M., Ramesh, K., Kumar, S. (2023). A mini-review on cryogenic carbon capture technology. *Frontiers in Energy Research*. https://www.frontiersin.org/articles/10.3389/fenrg.2023.1167099

16 Kenbay, A.A., Yerezhep, D.E., Aldiyarov, A.U. (2025). Development of low-temperature cell for IR Fourier-spectroscopy of hydrocarbon materials. *Eurasian phys. tech. j*., 22(2), 88–96. https://doi.org/10.31489/2025N2/88-96

17 Aminnaji, M., Hassanpouryouzband, A., Yang, J. (2024). CO_2 gas hydrate for carbon capture and storage applications. *Energy* 300, 131579. https://www.sciencedirect.com/science/article/pii/S0360544224013525

18 Wang, Y., Li, X., Zhao, J. (2025). Recent advances in CH_4 recovery from CH_4 hydrate in porous media by CO_2 replacement. *Energies*, 18(21), 5683. https://www.mdpi.com/1996-1073/18/21/5683

19 Amato, Z., Gärtner, S., Ghesquière, P., et al. (2026). Molecular and pore-scale structure evolution in amorphous solid water. Phys. Chem. Chem. Phys. 28, 524–537. https://doi.org/10.1039/D5CP03851K

20 Talewar, S.K., Halukeerthi, S.O., Riedlaicher, R., et al. (2019). Gaseous nanoprobes for detecting gas-trapping environments in macroscopic films of vapor-deposited amorphous ice. J. Chem. Phys. 151, 134505. https://doi.org/10.1063/1.5113505

21 Carmack, R.A., Tribbett, P.D., Loeffler, M.J. (2023). Pore Accessibility in Amorphous Solid Water. Astrophys. J., 942(1), 1. https://doi.org/10.3847/1538-4357/aca76b

22 Fukazawa, H., Kouchi, A., Hama, T., et al. (2025). Crystallization Mechanisms of Porous and Compact Amorphous Solid Water Films. Cryst. Growth Des., 25 (4), 1528-7483. https://doi.org/10.1021/acs.cgd.4c01284

23 Golikov O., Yerezhep D., Akylbayeva A., Sokolov D., Korshikov E., Nurmukan A., Aldiyarov A. (2023). Cryovacuum setup for optical studies of astrophysical ice. *Scientific Reports*, 13, 48541. https://doi.org/10.1038/s41598-023-48541-3

24 Yuan, C., Smith, R.S., Kay, B.D. (2016). Surface and bulk crystallization of amorphous solid water films: Confirmation of top-down crystallization. *Surface Science*, 652, 350–354. https://doi.org/10.1016/j.susc.2015.12.037

25 Mate, B., Cazaux, S., Satorre, M. A., Molpeceres, G., Ortigoso, J., Millan, C., & Santonja, C. (2020). *Diffusion of CH_4 in amorphous solid water*. Astronomy & Astrophysics, 643, A163. https://doi.org/10.1051/0004-6361/202038705

26 Amato, Z., Headen, T.F., Ghesquière, P., Fraser, H.J. (2025). A molecular dynamics study of the effect of annealing temperature on the structure of amorphous solid water. *Physical Chemistry Chemical Physics*, 27, 11186–11195. https://doi.org/10.1039/d5cp00271k

---

AUTHORS' INFORMATION

Chigambayeva, Nurgul Nurbayevna - Doctoral student, al-Farabi Kazakh National University Almaty, Kazakhstan; ORCID iD: 0009-0000-3753-3618; nurgul050490@gmail.com

Nurmukan, Assel Yerzhumayevna - PhD, Senior Lecturer, Department of Thermophysics and Technical Physics, al-Farabi Kazakh National University Almaty, Kazakhstan; SCOPUS Author ID: 57217033769; ORCID ID: 0000-0002-4231-0766; assel.nurmukan@kaznu.kz

Aldiyarov, Abdurahman Ualievich – Candidate of Physical and Mathematical Sciences, Acting Professor, Department of Thermophysics and Technical Physics, al-Farabi Kazakh National University Almaty, Kazakhstan; SCOPUS Author ID: 16201950600, ORCID ID: 0000-0002-5091-7699, Abdurakhman.Aldiyarov@kaznu.edu.kz

Korshikov Yevgeniy Sergeevich - PhD, Senior Lecturer, Department of Thermophysics and Technical Physics, al-Farabi Kazakh National University Almaty, Kazakhstan; Scopus Author ID: 55319247600; ORCID ID: 0000-0002-9479-4192, e.s.korshikov@physics.kz

Erlanov Timur Erlanovich - Master's student, al-Farabi Kazakh National University Almaty, Kazakhstan; ORCID ID: 0000-0003-4034-6981, yerlanovtimur@gmail.com